

Magnetic coupling of ferromagnetic SrRuO₃ epitaxial layers separated by ultrathin non-magnetic SrZrO₃/SrIrO₃

Lena Wysocki, Ramil Mirzaaghayev, Michael Ziese, Lin Yang, Jörg Schöpf, Rolf B. Versteeg, Andrea Bliesener, Johannes Engelmayer, András Kovács, Lei Jin, Felix Gunkel, Regina Dittmann, Paul H. M. van Loosdrecht, and Ionela Lindfors-Vrejoiu

Citation: *Appl. Phys. Lett.* **113**, 192402 (2018); doi: 10.1063/1.5050346

View online: <https://doi.org/10.1063/1.5050346>

View Table of Contents: <http://aip.scitation.org/toc/apl/113/19>

Published by the [American Institute of Physics](#)

Articles you may be interested in

[Creation of a thermally assisted skyrmion lattice in Pt/Co/Ta multilayer films](#)

Applied Physics Letters **113**, 192403 (2018); 10.1063/1.5053983

[Large electric field modulation of magnetic anisotropy in MgO/CoFe/Ta structures with monolayer oxide insertion](#)

Applied Physics Letters **113**, 192404 (2018); 10.1063/1.5043443

[Effect of epitaxial strain and vacancies on the ferroelectric-like response of CaTiO₃ thin films](#)

Applied Physics Letters **113**, 182902 (2018); 10.1063/1.5053857

[Exchange coupling in FeCoB/Ru, Mo/FeCoB trilayer structures](#)

Applied Physics Letters **113**, 192407 (2018); 10.1063/1.5045697

[Reduced interfacial magnetic moment of Y₃Fe₅O₁₂ by capping Pt](#)

Applied Physics Letters **113**, 182402 (2018); 10.1063/1.5046763

[Hall effect of asymmetric La_{0.7}Sr_{0.3}MnO₃/SrTiO₃/SrRuO₃ and La_{0.7}Sr_{0.3}MnO₃/BaTiO₃/SrRuO₃ superlattices](#)

Journal of Applied Physics **124**, 163905 (2018); 10.1063/1.5051812



MMR
TECHNOLOGIES

**THE WORLD'S RESOURCE FOR
VARIABLE TEMPERATURE
SOLID STATE CHARACTERIZATION**



WWW.MMR-TECH.COM

OPTICAL STUDIES SYSTEMS SEEBECK STUDIES SYSTEMS MICROPROBE STATIONS HALL EFFECT STUDY SYSTEMS AND MAGNETS

Magnetic coupling of ferromagnetic SrRuO₃ epitaxial layers separated by ultrathin non-magnetic SrIrO₃/SrIrO₃

Lena Wysocki,¹ Ramil Mirzaaghaev,¹ Michael Ziese,² Lin Yang,¹ Jörg Schöpf,¹ Rolf B. Versteeg,¹ Andrea Bliesener,¹ Johannes Engelmayer,¹ András Kovács,³ Lei Jin,³ Felix Gunkel,^{4,5} Regina Dittmann,⁴ Paul H. M. van Loosdrecht,¹ and Ionela Lindfors-Vrejoiu^{1,a)}

¹*II. Physikalisches Institut, Universität zu Köln, D-50937 Köln, Germany*

²*Division of Superconductivity and Magnetism, Felix Bloch Institute for Solid State Physics, University of Leipzig, D-04103 Leipzig, Germany*

³*Ernst Ruska-Centre and Peter Grünberg Institut (PGI-5), Forschungszentrum Jülich GmbH, D-52425 Jülich, Germany*

⁴*Peter Grünberg Institut (PGI-7), Forschungszentrum Jülich GmbH, D-52425 Jülich, Germany*

⁵*Institute of Electronic Materials (IWE2), RWTH Aachen University, D-52062 Aachen, Germany*

(Received 30 July 2018; accepted 17 October 2018; published online 6 November 2018)

Ferromagnetic multilayers with asymmetric interfaces and perpendicular magnetic anisotropy can stabilize non-trivial magnetic structures due to interfacial Dzyaloshinskii-Moriya interactions. Magnetic interlayer coupling between ferromagnetic layers separated by non-magnetic insulating spacers is an additional important ingredient for the properties of multilayers. We addressed the magnetic coupling between ferromagnetic SrRuO₃ epitaxial layers separated by ultrathin spacers of SrIrO₃/SrZrO₃, so that inversion symmetry is broken at the top and bottom interfaces. Major and minor magnetization loops allowed us to assess the type and strength of the magnetic coupling. We inferred that the magnetic coupling of SrRuO₃ layers through non-magnetic insulating interlayers (≤ 1.6 nm thick) is weakly ferromagnetic. © 2018 Author(s). All article content, except where otherwise noted, is licensed under a Creative Commons Attribution (CC BY) license (<http://creativecommons.org/licenses/by/4.0/>). <https://doi.org/10.1063/1.5050346>

In epitaxial heterostructures interfacial reconstructions, structural accommodations and interlayer coupling occur, which, together with the broken inversion symmetry, strongly influence their properties, often resulting in fascinating physical properties.^{1,2} In the particular case of magnetic multilayers, the type (ferromagnetic or antiferromagnetic) and the strength of magnetic interlayer coupling are key ingredients for tailoring their magnetic properties. Exchange interlayer coupling was extremely instrumental in metal multilayers with a ferromagnetic layer (for example, Co) sandwiched between two different heavy metals with large spin-orbit coupling (such as Ru, Pt, Pd, Ir, or Ta).^{3–6} Growth of multilayers with tailored repeats of Pt/Co/Ir trilayers or Co/Pd stabilized columnar skyrmions (< 100 nm diameter) at room temperature (RT), through dipolar interactions and/or interlayer exchange coupling (IEC).^{3–6} Furthermore, skyrmions formed at RT without any external magnetic field in thin Fe/Ni bilayers that were exchange-coupled to a thick bottom Ni layer through an optimally thick non-magnetic Cu spacer layer.⁷

Magnetic interlayer coupling in multilayers of ferromagnetic metals separated by non-magnetic metal spacers has been thoroughly studied experimentally and theoretically.^{8–10} When the ferromagnetic layers are interspaced with a thin insulator film, the nature of the interlayer interaction changes. In this case, the IEC arises from the spin-dependent electron-tunneling process, which causes the

coupling strength to decay monotonically as the thickness of the insulating spacer increases.^{11–16} So far, only a few studies have been devoted to the magnetic interlayer coupling in ferromagnetic perovskite epitaxial heterostructures, motivated primarily by the prospect of ferromagnetic tunnel junction devices. These heterostructures employ most often La_{1-x}Sr_xMnO₃ as ferromagnetic electrodes¹⁷ and much more rarely SrRuO₃,^{18,19} chiefly because the latter has a lower Curie temperature. Herranz *et al.* studied the interlayer coupling between two SrRuO₃ layers separated by non-magnetic insulating SrTiO₃ spacer layers and found that for a 2.5 nm thick spacer, the two magnetic layers were magnetically decoupled.¹⁸ Heterostructures of La_{0.7}Sr_{0.3}MnO₃ and SrRuO₃ that were separated by 0.4–0.8 nm thick SrTiO₃ layers were also only weakly ferromagnetically coupled.²⁰

Here, we study the type and the strength of magnetic interlayer coupling between ferromagnetic SrRuO₃ layers in multilayers with asymmetric interfaces. The motivation for growing such three-component heterostructures is to explore if we can have interfacial Dzyaloshinskii-Moriya interaction (DMI) at asymmetric interfaces between the ferromagnetic SrRuO₃ and materials with strong spin-orbit coupling such as SrIrO₃. Additive DMI can be obtained in multilayers in which DMI of opposite signs occurs at both upper and lower interfaces, as demonstrated for metallic dipolar-coupled asymmetric multilayers of Pt/Co/Ir.^{3,4} Recently, the formation of skyrmions in SrRuO₃/SrIrO₃ bilayers was proposed by Matsuno *et al.*²¹ Interfacial DMI due to inversion symmetry breaking and the large spin-orbit coupling of SrIrO₃ may result in non-collinear magnetic order in ultrathin SrRuO₃

^{a)} Author to whom correspondence should be addressed: vrejoiu@ph2.uni-koeln.de

layers with perpendicular magnetic anisotropy. It was further proposed that multilayers with ultrathin SrRuO₃ layers sandwiched between two different non-magnetic large spin-orbit coupling oxides may also form magnetic skyrmions.²² Electric field-manipulation of topological spin structures in epitaxial oxide heterostructures is the main driving force in the patent application from Ref. 22. In order to achieve this, topological magnetic textures have to be stabilized in materials that are insulating or poorly conducting metals. In contrast to ferromagnetic metals (Co, Ni, Fe), ferromagnetic perovskite oxides have the great advantage of showing thickness tunable-properties, such as metal-insulator transitions when their thickness is reduced to few monolayers (MLs), being thus more suitable for electric field effects. Moreover, the possibility of tailoring the oxygen octahedral tilt angles by interfacing perovskites with dissimilar tilts can be instrumental for yielding interfacial interactions and magnetic properties that are not exhibited by the bulk compounds.²³

Hence, assuming that skyrmions could form in ferromagnetic ultrathin SrRuO₃ layers, we are interested to answer the question whether in SrRuO₃/SrIrO₃/SrZrO₃ asymmetric multilayers skyrmions would couple across the non-magnetic insulating spacer. Magnetic interlayer coupling in such SrRuO₃ multilayers has prime importance for the study of topological magnetic domains in this material system, especially for magnetic imaging studies.

We designed samples with two SrRuO₃ layers of different thicknesses separated by a spacer consisting of a SrIrO₃/SrZrO₃ bilayer [see Fig. 1(a)], for investigating heterostructures that allow the evaluation of the interlayer coupling. The SrIrO₃ and SrZrO₃ layers of the heterostructure are 1 or 2 monolayers (MLs) thick each. Bulk SrZrO₃ is an insulating material, being a large band-gap dielectric at all temperatures. Bulk SrIrO₃ is a paramagnetic metal. It has been reported that ultrathin SrIrO₃ layers grown on SrTiO₃ have a transition from a semi-metallic to a correlated insulating state at about 4 ML thickness.²⁴ Hence, the SrRuO₃ layers of the heterostructures are separated either by a 2 ML or by a 4 ML (that is 0.8 nm or 1.6 nm thick) insulating spacer. The same 2 or 4 ML thick SrIrO₃/SrZrO₃ bilayer is used for capping the surface of the corresponding sample [see Fig. 1(a)]. The two SrRuO₃ layers of the heterostructures deliberately

have significantly different thicknesses, namely, 6 MLs for the top layer and 18 MLs for the bottom layer, so that their Curie temperatures T_C and coercive fields are sizably different over an extended temperature range.²⁵ The different coercive fields allow us to measure whether the two SrRuO₃ layers of our heterostructures are magnetically coupled. This is done by acquiring major and minor field-dependent magnetization $M(H)$ loops and by evaluating the shifts between the reversal fields for the magnetization of the layer with lower coercivity.¹⁴ We found that SrRuO₃ layers separated by 4 ML thick (≈ 1.6 nm) non-magnetic spacers have a weak ferromagnetic interlayer coupling of $\approx 18 \mu\text{J}/\text{m}^2$ at 10 K, compared to values such as $200 \mu\text{J}/\text{m}^2$, measured in strongly coupled Co/Ru multilayers¹⁰ at RT, or $2000 \mu\text{J}/\text{m}^2$ calculated for other systems.¹³ The coupling strength is $J_{IC} \approx 35 \mu\text{J}/\text{m}^2$ at 10 K for a sample with the thinnest spacer that we can grow (that is a SrIrO₃/SrZrO₃ bilayer with 1 ML thick individual layers).

The heterostructures were fabricated by pulsed-laser deposition (PLD) with a KrF excimer laser. Three stoichiometric ceramic targets of SrRuO₃, SrIrO₃, and SrZrO₃ were employed for the PLD growth. The heterostructures were deposited on SrTiO₃(100) single-crystal substrates. The details about sample growth are given in the [supplementary material](#). The growth mode was monitored by high oxygen pressure reflective high-energy electron diffraction (RHEED). Under our PLD conditions, the SrRuO₃ layers grew in a step-flow growth regime,²⁶ while the SrIrO₃ and SrZrO₃ grew in a layer-by-layer mode (see [supplementary material](#), Fig. S1), resulting in a smooth topography that preserved the step-and-terrace morphology of the substrate [Fig. 1(c)], with only mild step bunching [Fig. 1(d)]. The microstructure and the quality of the interfaces were investigated by scanning transmission electron microscopy (STEM) of cross-sectional specimens. High angle annular dark field (HAADF)-STEM imaging was performed at 200 kV on an FEI Titan 80–200 ChemiSTEM microscope. Figure 1(b) shows a HAADF-STEM micrograph of a heterostructure such as in Fig. 1(a), with 2 ML SrIrO₃ and 2 ML SrZrO₃ layers forming the spacer and capping. HAADF-STEM was used in conjunction with the RHEED for the calibration of the layer thickness (see [supplementary material](#), Fig. S2).

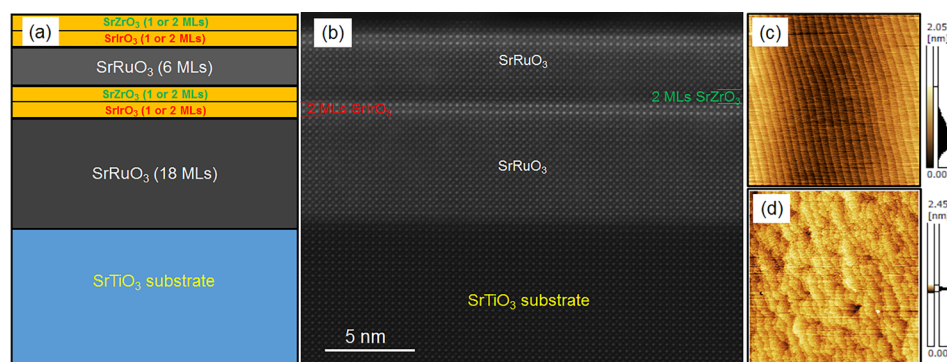


FIG. 1. Heterostructure employed for the investigation of the magnetic interlayer coupling between SrRuO₃ layers grown on a vicinal SrTiO₃(100) substrate, with two SrRuO₃ layers of different thicknesses: (a) sample schematics and (b) HAADF-STEM cross-sectional image of a test sample with 2 ML SrIrO₃ and 2 ML SrZrO₃ spacer and capping layers. AFM topography images ($5 \mu\text{m} \times 5 \mu\text{m}$ scan size) show in (c) the top surface of a substrate after etching and annealing and in (d) the top surface of the heterostructure with 2 ML SrIrO₃/SrZrO₃ spacer and capping layers, exhibiting the step-and-terrace morphology inherent to the vicinal substrate.

Magnetization measurements were performed with a superconducting quantum interference device (SQUID) magnetometer (MPMS XL7 from Quantum Design, magnetic field up to 7 T).

Magneto-optic Kerr effect (MOKE) measurements were performed in polar geometry, with the magnetic field perpendicular to the heterostructure surface, probing with incoherent light at a wavelength of 540 nm, with a 10 nm bandwidth.

To determine the Curie temperatures of the two ferromagnetic SrRuO₃ layers, we measured the temperature dependence of the magnetization of the heterostructure with 4 ML thick spacer and capping layers. The magnetization was measured with a magnetic field of 0.1 T applied perpendicular to the sample surface while the sample was heated, after being field-cooled (also in 0.1 T), from room temperature down to 3 K. Epitaxial SrRuO₃ layers grown on SrTiO₃(100) have out-of-plane magnetic anisotropy and ferromagnetic Curie temperature $T_C \approx 150$ K.^{25,27,28} Two ordering transitions were apparent in the magnetization as a function of temperature, marked by the arrows as shown in Fig. 2(a). The more accurate determination of the Curie temperature by calculating the first derivative of the magnetization as a function of temperature yields 138 K for the bottom 18 ML SrRuO₃ and 120 K for the top 6 ML SrRuO₃ [see the inset in Fig. 2(a)]. In Fig. 2(b), we show the temperature dependence of the major magnetization loops. Below 30 K, the major M(H) loops show clearly two steps corresponding to the magnetization reversal of the two layers at different fields. The layer with larger magnetization (that is the bottom 18 ML SrRuO₃) is responsible for the step at lower field in the M(H) loops. We found that around 50 K, the two layers

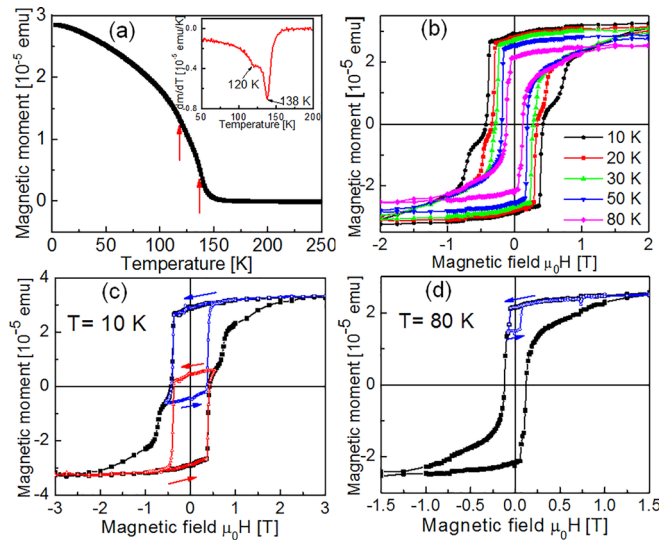


FIG. 2. SQUID magnetometry investigations of the temperature and field dependence of the magnetization of the heterostructure with 4 ML thick spacer and capping layers: (a) Field-cooled (0.1 T) magnetization as a function of temperature; (b) major magnetization loops at temperatures from 10 K to 80 K, (c) major loop at 10 K and two minor loops between saturated states in ± 5 T and reversal fields of ± 0.55 T; (d) major loop at 80 K and a minor loop between saturation and reversal field of -0.083 T. The magnetic field was applied perpendicular to the heterostructure surface for all measurements. The inset in (a) shows the first derivative of the magnetization with respect to temperature, to determine the Curie temperatures for the two SrRuO₃ layers of the heterostructure: $T_C = 120$ K for the 6 ML top layer and $T_C = 138$ K for the 18 ML bottom layer.

have almost the same values of the reversal field. At 80 K, the 6 ML SrRuO₃ layer has a lower switching field and will thus reverse its magnetization first, as a first sharp step of lower height is observed in the major loop at about 0.065 T. This is the consequence of different temperature dependence of the coercive fields of the 18 ML thick and 6 ML thick SrRuO₃ layers (see more details in the [supplementary material](#)). We calculated the saturation magnetic moment in μ_B/Ru at 10 K, using a total thickness of 24 MLs of SrRuO₃ in the heterostructure. It has an *average* value of $1.4 \mu_B/\text{Ru}$, which is lower than the $1.9 \mu_B/\text{Ru}$ of our 40 nm thick (≈ 100 MLs) epitaxial SrRuO₃.^{27,28} We assume that the magnetic moment of the 18 ML SrRuO₃ layer is higher than the average value of $1.4 \mu_B/\text{Ru}$ and the magnetic moment of the 6 ML SrRuO₃ layer is lower than this average value. The saturation magnetic moment at 10 K for a 4 ML SrRuO₃ film was reported to be $1.2 \mu_B/\text{Ru}$.²⁸

To assess the type and strength of the coupling, both major and minor M(H) loops were measured at several temperatures below the ordering temperature of both layers. Major and minor hysteresis loops at 10 K are displayed in Fig. 2(c). The major loop clearly exhibited two sharp magnetization reversal steps and a tail at high fields, before reaching saturation. Decreasing the field from saturation in 5 T and reversing the polarity, a first magnetization step occurred at -0.396 T and corresponds to the magnetization switching of the major part of the bottom 18 ML SrRuO₃ layer. The second step was at about -0.74 T and it is due to the magnetization switching in the top 6 ML SrRuO₃ layer. The values of the switching fields at 10 K are in good agreement with the values for bare SrRuO₃ layers of similar thicknesses grown on SrTiO₃(100) reported in Ref. 25 and with the values we obtained for reference samples (see [supplementary material](#), Fig. S3). By comparison with a reference sample consisting of an 18 ML SrRuO₃ layer grown on SrTiO₃ and capped with a 4 ML SrIrO₃/SrZrO₃ bilayer (see [supplementary material](#), Fig. S3), we assign the tail of the major loop (for field values larger than about 1 T) chiefly to the saturation of the magnetization of the bottom 18 ML SrRuO₃ layer. Most likely a minor fraction of possibly strongly pinned domains with magnetization antiparallel to the applied field requires large field values (almost 3 T) to be annihilated and saturation is only gradually reached. Two minor loops were measured between saturation at ± 5 T and reversal of the magnetization of the bottom layer at ∓ 0.55 T [Fig. 2(c)]. For both minor loops, the magnetization reversal on the way back to saturation in high fields occurred at a slightly smaller field value of about ± 0.38 T, respectively. Hence, the magnitude of the shift is 16 mT, which is 5% of the difference between the two switching fields at 10 K. This shows that a ferromagnetic coupling exists between the two SrRuO₃ layers separated by a 4 ML spacer and as the magnitude of the shift is small, the magnetic coupling appears to be weak. The shift of the minor loop becomes very small at 80 K, about 3 mT, almost at the limit of our detection [Fig. 2(d)]. We compared the SQUID magnetometry M(H) results with polar magneto-optic Kerr effect (MOKE) measurements. We measured Kerr rotation major and minor loops and, similar to the SQUID measurements, we evaluated the shifts of the minor loops. The shifts showed good agreement

with the shifts yielded by the SQUID minor loops (see [supplementary material](#), Fig. S4). In addition, the MOKE investigations allowed us to measure the temperature dependence of the reversal fields for the two SrRuO₃ layers.

For the determination of the strength of the interlayer coupling, J_{IC} , we followed the procedure described in detail by van der Heijden *et al.* in their study of the coupling between two ferromagnetic Fe₃O₄ layers separated by insulating non-magnetic MgO layer.¹⁴ The J_{IC} between two epitaxial ferromagnetic Fe₃O₄ layers with full in-plane magnetization separated by a spacer of similar thickness as in our heterostructures (1.3 nm MgO spacer layer) was 50 $\mu\text{J}/\text{m}^2$ at RT.¹⁴ Using Eqs. (1a) and (1b) proposed in Ref. 14, we estimated the interlayer coupling strength J_{IC} as 18 $\mu\text{J}/\text{m}^2$ at 10 K (see [supplementary material](#) for details, especially for the discussion on the validity of our estimations). In comparison with the J_{IC} of magnetite layers separated by MgO given above or with the ferromagnetic coupling strength of Co/Ru/Co with 1.2 nm thick Ru (200 $\mu\text{J}/\text{m}^2$ at RT),¹⁰ the interlayer coupling between SrRuO₃ layers separated by 4 ML SrZrO₃/SrIrO₃ is comparably weak. Further supportive data for the weak ferromagnetic interlayer coupling, by comparison with reference SrRuO₃ single layers, are shown in the [supplementary material](#).

We also investigated a heterostructure with two SrRuO₃ layers for which the spacer and the capping were in total 2 ML thick (≈ 0.8 nm) SrZrO₃/SrIrO₃ bilayers, which is the lowest thickness that we can achieve for the spacer in our asymmetric heterostructures. Major and minor SQUID magnetization loops at 10 K are displayed in Fig. 3. The major loop exhibited two sharp magnetization reversal steps, similar to the M(H) loop of the heterostructure with a 4 ML thick spacer. Decreasing the field from saturation in 5 T and reversing the polarity, a first magnetization reversal step occurred at -0.31 T and corresponds to the magnetization reversal of the bottom 18 ML SrRuO₃ layer. The second step was at -0.53 T, and it is due to the magnetization switching in the top 6 ML SrRuO₃ layer. We note that the 6 ML SrRuO₃ layer of this heterostructure has a much lower switching field than the 6 ML layer of the heterostructure with a 4 ML spacer (0.74 T at 10 K) or of the 6 ML SrRuO₃

reference sample (see [supplementary material](#)). This is in accord with a stronger ferromagnetic interlayer coupling in this heterostructure, resulting in the reduction of the coercive field of the harder layer.¹⁴ A minor loop was measured between saturation in 5 T and reversal of the magnetization of the magnetically softer layer at -0.425 T. For the minor loop, the magnetization reversal under positive field took place also at a slightly smaller field value of 0.28 T. The magnitude of the shift is 30 mT (see inset in Fig. 3), which is 14% of the difference between the switching fields of the two SrRuO₃ layers at 10 K. This shows that the coupling between the two SrRuO₃ layers separated by a 2 ML spacer is ferromagnetic and still relatively weak. It is larger though than for the heterostructure with a thicker spacer (estimated $J_{IC} \approx 35$ $\mu\text{J}/\text{m}^2$). The larger ferromagnetic coupling strength between the SrRuO₃ layer separated by the thinner 2 ML spacer is expectable, if the coupling is primarily due to tunneling of spin-polarized electrons across the insulating non-magnetic barrier;^{11,12} however, we cannot pinpoint the main coupling mechanism based on the current data. Additionally, the indirect coupling due to pinholes in the spacer is probably more effective in the case of the 2 ML thick spacer.^{12,14,15,29} We stress that the spacer is inhomogeneous (either 1 ML SrIrO₃/1 ML SrZrO₃ or 2 ML SrIrO₃/2 ML SrZrO₃) and therefore the physical properties of the barrier, relevant for spin-polarized electron tunneling, may not scale with the thickness in a trivial manner. Furthermore, interfacial interactions may affect the electronic band structure of the metallic SrRuO₃ layers differently when the thickness of the SrIrO₃ layers increases.

Summarizing, we studied the magnetic interlayer coupling between epitaxial SrRuO₃ layers with perpendicular magnetic anisotropy, in SrRuO₃/SrIrO₃/SrZrO₃ multilayers grown on SrTiO₃(100) substrates. For 2 and 4 ML thick SrIrO₃/SrZrO₃ epitaxial insulating spacers, the two ferromagnetic SrRuO₃ layers are almost decoupled, exhibiting only a very weak ferromagnetic coupling of the order of 35 $\mu\text{J}/\text{m}^2$ at 10 K. Therefore, we expect that nucleation and growth of magnetic domains upon magnetization reversal in the individual ferromagnetic layers of SrRuO₃/SrIrO₃/SrZrO₃ multilayers will proceed layer-independently. The weak magnetic coupling between the SrRuO₃ layers is unfavorable for the generation of coupled topological magnetic textures, such as the columnar skyrmions generated in dipolar-coupled asymmetric Pt/Co/Ir multilayers.^{3,4} In SrRuO₃/SrIrO₃/SrZrO₃ or similar multilayers (see, for example, the patent application in Ref. 22), skyrmions will form at different locations and have only accidental correlations in the uncoupled ferromagnetic SrRuO₃ layers. This makes the imaging of the magnetic domains or skyrmions and also their manipulation and monitoring challenging. However, such asymmetric multilayers may have the potentially great advantage of enlarged (additive) interfacial Dzyaloshinskii-Moriya interactions, which can significantly reduce the size of the magnetic domains with non-trivial topology. Furthermore, the increased magnetic volume in multilayers may reinforce the stability of metastable magnetic domains against thermal fluctuations and thus expand their temperature stability range closer to the Curie temperature of SrRuO₃ layers.³

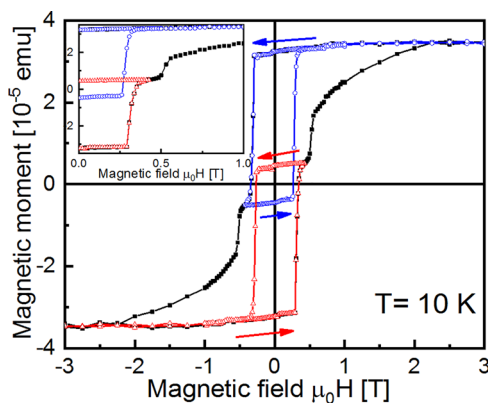


FIG. 3. SQUID magnetization loops of the heterostructure with 2 ML thick (≈ 0.8 nm) spacer and capping SrIrO₃/SrZrO₃ layers: major loop and two minor loops between saturated states and reversal fields of ± 0.425 T, measured at 10 K. The inset shows a zoom-in of the first and fourth quadrants to display better the shift between the minor loop and the major loop.

See [supplementary material](#) for details about the sample growth and structural characterization, for additional SQUID magnetization data of reference single SrRuO₃ layers samples, and for MOKE measurements of the heterostructures used for the interlayer coupling study.

We thank René Borowski (FZ Jülich) for etching the substrates and Susanne Heijligen (University of Cologne) for assistance with SQUID magnetometry. Insightful suggestions from Achim Rosch (University of Cologne) were very helpful. Financial support from German Research Foundation (Project Nos. LI 3015/3-1 and LI 3015/5-1), and through Nos. SFB 1238 and SPP 2137, and from the German Excellence Initiative via the key profile area “quantum matter and materials” of the University of Cologne is gratefully acknowledged.

- ¹P. Zubko, S. Gariglio, M. Gabay, P. Ghosez, and J.-M. Triscone, *Annu. Rev. Condens. Matter Phys.* **2**, 141 (2011).
- ²H. Y. Hwang, Y. Iwasa, M. Kawasaki, B. Keimer, N. Nagaosa, and Y. Tokura, *Nat. Mater.* **11**, 103 (2012).
- ³C. Moreau-Luchaire, C. Moutafis, N. Reyren, J. Sampaio, C. A. F. Vaz, N. Van Horne, K. Bouzehouane, K. Garcia, C. Deranlot, P. Warnicke, P. Wohlhüter, J.-M. George, M. Weigand, J. Raabe, V. Cros, and A. Fert, *Nat. Nanotechnol.* **11**, 444 (2016).
- ⁴A. Soumyanarayanan, M. Raju, A. L. Gonzalez Oyarce, A. K. C. Tan, M.-Y. Im, A. P. Petrović, P. Ho, K. H. Khoo, M. Tran, C. K. Gan, F. Ernult, and C. Panagopoulos, *Nat. Mater.* **16**, 898 (2017).
- ⁵A. K. Nandy, N. S. Kiselev, and S. Blügel, *Phys. Rev. Lett.* **116**, 177202 (2016).
- ⁶S. D. Pollard, J. A. Garlow, J. Yu, Z. Wang, Y. Zhu, and H. Yang, *Nat. Commun.* **8**, 14761 (2017).
- ⁷G. Chen, A. Masacraque, A. T. N'Diaye, and A. K. Schmid, *Appl. Phys. Lett.* **106**, 242404 (2015).
- ⁸S. S. P. Parkin, R. Bhadra, and K. P. Roche, *Phys. Rev. Lett.* **66**, 2152 (1991).
- ⁹P. Bruno, *Phys. Rev. B* **52**, 411 (1995).
- ¹⁰P. J. H. Bloemen, H. W. van Kesteren, H. J. M. Swagten, and W. J. M. de Jonge, *Phys. Rev. B* **50**, 13505 (1994).
- ¹¹J. C. Slonczewski, *Phys. Rev. B* **39**, 6995 (1989).
- ¹²J. Faure-Vincent, C. Tiusan, C. Bellouard, E. Popova, M. Hehn, F. Montaigne, and A. Schuhl, *Phys. Rev. Lett.* **89**, 107206 (2002).
- ¹³S. Wang, K. Xia, T. Min, and Y. Ke, *Phys. Rev. B* **96**, 024443 (2017).
- ¹⁴P. A. A. van der Heijden, P. J. H. Bloemen, J. M. Metselaar, R. M. Wolf, J. M. Gaines, J. T. W. M. van Eemeren, P. J. van der Zaag, and W. J. M. de Jonge, *Phys. Rev. B* **55**, 11569 (1997).
- ¹⁵C. L. Platt, M. R. McCartney, F. T. Parker, and A. E. Berkowitz, *Phys. Rev. B* **61**, 9633 (2000).
- ¹⁶Y. Ijiri, *J. Phys.: Condens. Matter* **14**, R947 (2002).
- ¹⁷M. Bowen, M. Bibes, A. Barthélémy, J.-P. Contour, A. Anane, Y. Lemaître, and A. Fert, *Appl. Phys. Lett.* **82**, 233 (2003).
- ¹⁸G. Herranz, B. Martínez, J. Fontcuberta, F. Sánchez, M. V. García-Cuenca, C. Ferrater, and M. Varela, *J. Appl. Phys.* **93**, 8035 (2003).
- ¹⁹K. S. Takahashi, A. Sawa, Y. Ishii, H. Akoh, M. Kawasaki, and Y. Tokura, *Phys. Rev. B* **67**, 094413 (2003).
- ²⁰M. Ziese, I. Vrejoiu, E. Pippel, P. Esquinazi, D. Hesse, C. Etz, J. Henk, A. Ernst, I. V. Maznichenko, W. Hergert, and I. Mertig, *Phys. Rev. Lett.* **104**, 167203 (2010).
- ²¹J. Matsuno, N. Ogawa, K. Yasuda, F. Kagawa, W. Koshibae, N. Nagaosa, Y. Tokura, and M. Kawasaki, *Sci. Adv.* **2**, e1600304 (2016).
- ²²M. Nakamura, J. Matsuno, M. Kawasaki, Y. Tokura, and Y. Kaneko, “Magnetic element, skyrmion memory, solid-state electronic device, data-storage device, data processing and communication device,” U.S. patent application 15/450,044 (2017).
- ²³S. Dong, Q. Zhang, S. Yunoki, J.-M. Liu, and E. Dagotto, *Phys. Rev. B* **84**, 224437 (2011).
- ²⁴D. J. Groenendijk, C. Autieri, J. Girovsky, M. C. Martinez-Velarte, N. Manca, G. Mattoni, A. M. R. V. L. Monteiro, N. Gauquelin, J. Verbeeck, A. F. Otte, M. Gabay, S. Picozzi, and A. D. Caviglia, *Phys. Rev. Lett.* **119**, 256403 (2017).
- ²⁵J. Xia, W. Siemons, G. Koster, M. R. Beasley, and A. Kapitulnik, *Phys. Rev. B* **79**, 140407(R) (2009).
- ²⁶J. Choi, C. B. Eom, G. Rijnders, H. Rogalla, and D. H. A. Blank, *Appl. Phys. Lett.* **79**, 1447 (2001).
- ²⁷M. Ziese, I. Vrejoiu, and D. Hesse, *Phys. Rev. B* **81**, 184418 (2010).
- ²⁸F. Bern, M. Ziese, A. Setzer, E. Pippel, D. Hesse, and I. Vrejoiu, *J. Phys.: Condens. Matter* **25**, 496003 (2013).
- ²⁹J. F. Bobo, H. Kikuchi, O. Redon, E. Snoeck, M. Piecuch, and R. L. White, *Phys. Rev. B* **60**, 4131 (1999).